JOURNAL OF AIRCRAFT
Vol. 45, No. 4, July–August 2008

Effects of Nonlinearities on Subsonic Aerodynamic Center

W. F. Phillips*
Utah State University, Logan, Utah 84322-4130
N. R. Alley†
Georgia Institute of Technology, Atlanta, Georgia 30332-0150
and
R. J. Niewoehner‡
U.S. Naval Academy, Annapolis, Maryland 21402-5025

DOI: 10.2514/1.34241

A refined mathematical definition for the aerodynamic center of a wing or complete airplane is presented, which allows for inclusion of the trigonometric and aerodynamic nonlinearities. From this definition, analytical relations are developed for both the axial and vertical positions of the aerodynamic center at any angle of attack, independent of whether or not the nonlinearities are included. Results show that, when all nonlinearities are included, the position of the aerodynamic center can change with angle of attack. Because the traditional approximation provides only a fixed axial coordinate, this analysis provides two additional pieces of information about the aerodynamic center, that is, its vertical coordinate and its movement. Two examples are presented, which separate these two effects. The first example uses computational fluid dynamics to show that, when the effects of the nonlinearities are combined with wing sweep at high angles of attack below stall, the aerodynamic center of a planar wing moves significantly aft and below the wing. The second example, which uses an approximate closed-form solution for two lifting surfaces, emphasizes the importance of knowing the vertical position of the aerodynamic center and shows that, in the absence of sweep, its movement with angle of attack is slight.

Nomenclature

b	=	wingspan
C	=	aerodynamic coefficient for wing or complete aircraft
$\tilde{C}$	=	local in situ wing section aerodynamic coefficient
c	=	local airfoil section chord length
$\bar{c}$	=	mean chord length
D	=	total drag for wing or complete aircraft, includes both parasitic and induced drag
$\tilde{D}$	=	local in situ wing section drag, includes both parasitic and induced drag
e	=	span efficiency factor
L	=	total lift for wing or complete aircraft
$\tilde{L}$	=	local in situ wing section lift
m	=	pitching moment for wing or complete aircraft
$\tilde{m}$	=	local in situ wing section pitching moment
R_A	=	aspect ratio, b^2/S
R_T	=	taper ratio, $c_{\text{tip}}/c_{\text{root}}$
S	=	planform area, horizontal projection
V_∞	=	magnitude of the freestream velocity
x	=	axial coordinate measured aft of aerodynamic center of root wing section or fuselage reference origin
$\tilde{x}$	=	axial coordinate of local wing section
$\bar{x}$	=	mean axial coordinate
y	=	normal coordinate measured above aerodynamic center of root wing section or fuselage reference origin
$\tilde{y}$	=	normal coordinate of local wing section
$\bar{y}$	=	mean normal coordinate
y^+	=	dimensionless normal shear coordinate at first grid point from surface
z	=	spanwise coordinate measured outboard from wing or aircraft plane of symmetry
$\bar{z}$	=	mean spanwise coordinate
α	=	geometric angle of attack relative to the freestream
Γ	=	quarter-chord dihedral angle
γ	=	climb angle
δ_e	=	elevator deflection angle
ε	=	downwash angle
θ	=	elevation angle
Λ	=	quarter-chord sweep angle
ρ_∞	=	freestream air density
Ω	=	maximum total twist angle, geometric plus aerodynamic

Subscripts

A	=	axial force
ac	=	aerodynamic center
c.g.	=	center of gravity
D	=	drag force
h	=	horizontal control surface
L	=	lift force
m	=	pitching moment
mac	=	mean aerodynamic chord
N	=	normal force
ref	=	arbitrary reference
w	=	main wing
α	=	angle of attack
ε	=	downwash angle
0	=	origin, zero lift, or zero-angle-of-attack contribution
,	=	derivative with respect to following subscript

Received 25 August 2007; revision received 14 January 2008; accepted for publication 14 January 2008.

*Professor, Mechanical and Aerospace Engineering Department, 4130 Old Main Hill. Senior Member AIAA.
†Research Engineer II, School of Aerospace Engineering, 270 Ferst Drive. Member AIAA.
‡Captain, U.S. Navy, Aerospace Engineering Department, 590 Holloway Road. Member AIAA.

Introduction

THE distribution of aerodynamic loads acting on a wing or complete aircraft can be replaced with a resultant force acting at the aerodynamic center and a resultant moment that does not vary with small changes in angle of attack. Because drag is typically small

compared with lift, drag is commonly neglected when estimating the position of the aerodynamic center at small angles of attack. See, for example, Etkin and Reid [1], McCormick [2], Pamadi [3], or Raymer [4]. Furthermore, the trigonometric functions that appear in the relation between lift and pitching moment are traditionally linearized using the approximations $\cos(\alpha) \approx 1$ and $\sin(\alpha) \approx \alpha$. Nevertheless, at larger angles of attack the nonlinearities associated with the trigonometric functions and the drag can significantly alter the position of the aerodynamic center of a wing or complete aircraft, even at angles of attack below stall. At poststall angles of attack, the position of the aerodynamic center may be dominated by nonlinear effects.

The aerodynamic center of an airfoil section is typically defined to be the point on the chord line about which the change in the pitching moment with respect to angle of attack is zero. The position of this aerodynamic center is nearly independent of angle of attack. Thin airfoil theory predicts that the subsonic aerodynamic center of any airfoil is the quarter chord, and experimental data show that the actual aerodynamic center of most airfoils is very near the quarter chord at low Mach numbers and small angles of attack.

For a finite wing or complete airplane, the aerodynamic center is traditionally defined to be the point about which the pitching moment is independent of angle of attack [1–3]. Furthermore, traditional formulations for the pitch-stability derivative tacitly neglect the change in position of the aerodynamic center with respect to angle of attack [1–4]. However, outside the approximation of linear aerodynamics, there may be no fixed point on a wing or complete aircraft about which the pitching moment is totally independent of the angle of attack. Thus, a less restrictive definition for the aerodynamic center is needed if we are to account for the trigonometric and aerodynamic nonlinearities.

In general, the aerodynamic center of a spanwise symmetric wing or complete airplane lies in the plane of symmetry and can be more precisely defined to satisfy two constraints.

1) The pitching moment about the aerodynamic center must be invariant to small changes in angle of attack:

$$\frac{\partial C_{m_{\text{ac}}}}{\partial \alpha} \equiv 0 \tag{1}$$

2) The location of the aerodynamic center must be invariant to small changes in angle of attack:

$$\frac{\partial \bar{x}_{\text{ac}}}{\partial \alpha} \equiv 0, \qquad \frac{\partial \bar{y}_{\text{ac}}}{\partial \alpha} \equiv 0 \tag{2}$$

Note that Eq. (1) does not necessarily require the pitching moment about the aerodynamic center to be independent of angle of attack, as is commonly stated. To require $C_{m_{\text{ac}}}$ to be independent of α, we would need to force all derivatives of $C_{m_{\text{ac}}}$ with respect to α to be zero, not just the first derivative. Because there are only 2 degrees of freedom associated with the position of the aerodynamic center, we cannot force $C_{m_{\text{ac}}}$ to be independent of α for an arbitrary wing or complete airplane. By similar reasoning, Eq. (2) does not require the position of the aerodynamic center to be independent of angle of attack. Although we are requiring the first derivative of $\bar{x}_{\text{ac}}$ and $\bar{y}_{\text{ac}}$ with respect to α to be zero, the higher-order derivatives may not be zero, allowing the position of the aerodynamic center to change with angle of attack.

To examine how the aerodynamic center can be located from Eqs. (1) and (2), we first consider the pitching moment developed by an arbitrary wing. From Fig. 1, the pitching moment about the origin, $x = 0$, $y = 0$, for a wing of arbitrary planform and dihedral can be written as

$$m_0 = \int_{z=-b/2}^{b/2} \tilde{m}_{\text{ac}}\,\mathrm{d}z - \int_{z=-b/2}^{b/2} (\tilde{L}\cos\alpha + \tilde{D}\sin\alpha)\tilde{x}_{\text{ac}}\,\mathrm{d}z - \int_{z=-b/2}^{b/2} (\tilde{L}\sin\alpha - \tilde{D}\cos\alpha)\tilde{y}_{\text{ac}}\,\mathrm{d}z \tag{3}$$

where $\tilde{x}_{\text{ac}}$ and $\tilde{y}_{\text{ac}}$ denote the x and y coordinates of the locus of wing section aerodynamic centers. Note that in Eq. (3), $\tilde{m}_{\text{ac}}$, $\tilde{L}$, and $\tilde{D}$ are

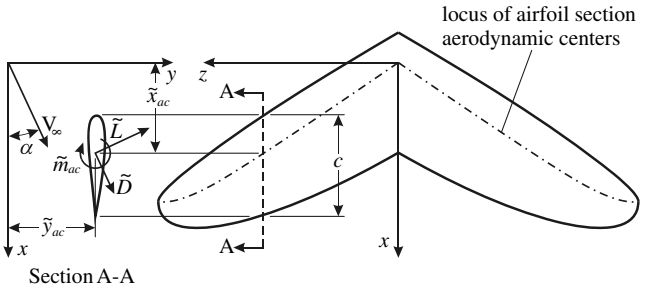

Fig. 1 Section lift, drag, and pitching moment acting on a section of an arbitrary wing.

section moment and force components per unit span, not per unit distance measured parallel with the local dihedral. Dividing Eq. (3) by dynamic pressure yields

$$\frac{m_0}{\frac{1}{2}\rho_\infty V_\infty^2} = \int_{z=-b/2}^{b/2} \tilde{C}_{m_{\text{ac}}} c^2\,\mathrm{d}z - \int_{z=-b/2}^{b/2} (\tilde{C}_L\cos\alpha + \tilde{C}_D\sin\alpha)c\tilde{x}_{\text{ac}}\,\mathrm{d}z - \int_{z=-b/2}^{b/2} (\tilde{C}_L\sin\alpha - \tilde{C}_D\cos\alpha)c\tilde{y}_{\text{ac}}\,\mathrm{d}z \tag{4}$$

In general, $\tilde{C}_{m_{\text{ac}}}$, $\tilde{C}_L$, $\tilde{C}_D$, c, $\tilde{x}_{\text{ac}}$, and $\tilde{y}_{\text{ac}}$ all vary with the spanwise coordinate z. Note that, as used in Eq. (4), $\tilde{C}_{m_{\text{ac}}}$, $\tilde{C}_L$, and $\tilde{C}_D$ are local in situ wing section aerodynamic coefficients, which include the effects of wing downwash. Thus, $\tilde{C}_L$ is reduced by the induced angle of attack and $\tilde{C}_D$ includes both parasitic and induced drag.

The wing reference area is traditionally taken to be the horizontal projected planform area, which for a spanwise symmetric wing can be written as

$$S \equiv \int_{z=-b/2}^{b/2} c\,\mathrm{d}z = 2\int_{z=0}^{b/2} c\,\mathrm{d}z \tag{5}$$

With this definition and the traditional definitions for the wing lift and drag coefficients, we now define what we shall call the semispan aerodynamic center of lift $(\bar{x}_L, \bar{y}_L, \bar{z}_L)$,

$$\bar{x}_L \equiv \frac{2}{C_L S}\int_{z=0}^{b/2} \tilde{C}_L c\tilde{x}_{\text{ac}}\,\mathrm{d}z, \qquad \bar{y}_L \equiv \frac{2}{C_L S}\int_{z=0}^{b/2} \tilde{C}_L c\tilde{y}_{\text{ac}}\,\mathrm{d}z$$
$$\bar{z}_L \equiv \frac{2}{C_L S}\int_{z=0}^{b/2} \tilde{C}_L cz\,\mathrm{d}z, \qquad C_L \equiv \frac{2}{S}\int_{z=0}^{b/2} \tilde{C}_L c\,\mathrm{d}z \tag{6}$$

and the semispan aerodynamic center of drag $(\bar{x}_D, \bar{y}_D, \bar{z}_D)$,

$$\bar{x}_D \equiv \frac{2}{C_D S}\int_{z=0}^{b/2} \tilde{C}_D c\tilde{x}_{\text{ac}}\,\mathrm{d}z, \qquad \bar{y}_D \equiv \frac{2}{C_D S}\int_{z=0}^{b/2} \tilde{C}_D c\tilde{y}_{\text{ac}}\,\mathrm{d}z$$
$$\bar{z}_D \equiv \frac{2}{C_D S}\int_{z=0}^{b/2} \tilde{C}_D cz\,\mathrm{d}z, \qquad C_D \equiv \frac{2}{S}\int_{z=0}^{b/2} \tilde{C}_D c\,\mathrm{d}z \tag{7}$$

Note that these definitions differ from the traditional definitions for the centers of lift and drag, because the section aerodynamic center is used in Eqs. (6) and (7) rather than the section center of pressure. In a similar manner, we define a mean section moment coefficient and the mean aerodynamic chord length

$$\bar{\tilde{C}}_{m_{\text{ac}}} \equiv \frac{2}{S\bar{c}_{\text{mac}}}\int_{z=0}^{b/2} \tilde{C}_{m_{\text{ac}}} c^2\,\mathrm{d}z, \qquad \bar{c}_{\text{mac}} \equiv \frac{2}{S}\int_{z=0}^{b/2} c^2\,\mathrm{d}z \tag{8}$$

Using these definitions and dividing by the planform area of the wing, Eq. (4) can be written as

$$C_{m_0} c_{\text{ref}} \equiv \frac{m_0}{\frac{1}{2}\rho_\infty V_\infty^2 S} = \bar{\tilde{C}}_{m_{\text{ac}}}\bar{c}_{\text{mac}} - C_L\bar{x}_L\cos\alpha - C_D\bar{x}_D\sin\alpha - C_L\bar{y}_L\sin\alpha + C_D\bar{y}_D\cos\alpha \tag{9}$$

where c_{ref} is the arbitrary reference length chosen to nondimensionalize the pitching moment coefficient.

The distributed aerodynamic loads acting on the wing can be replaced with a resultant force and moment acting at the aerodynamic center of the wing $(\bar{x}_{\text{ac}}, \bar{y}_{\text{ac}})$. Thus, the pitching moment about the origin can also be written as

$$m_0 = m_{\text{ac}} - \bar{x}_{\text{ac}}(L\cos\alpha + D\sin\alpha) - \bar{y}_{\text{ac}}(L\sin\alpha - D\cos\alpha) \quad (10)$$

where m_{ac} is the pitching moment about the aerodynamic center. Dividing by the dynamic pressure and planform area, Eq. (10) becomes

$$C_{m_0}c_{\text{ref}} = C_{m_{\text{ac}}}c_{\text{ref}} - \bar{x}_{\text{ac}}(C_L\cos\alpha + C_D\sin\alpha) - \bar{y}_{\text{ac}}(C_L\sin\alpha - C_D\cos\alpha) \quad (11)$$

Combining Eqs. (9) and (11) to eliminate the pitching moment coefficient about the origin and rearranging gives

$$\bar{x}_{\text{ac}}(C_L\cos\alpha + C_D\sin\alpha) + \bar{y}_{\text{ac}}(C_L\sin\alpha - C_D\cos\alpha) - C_{m_{\text{ac}}}c_{\text{ref}} = C_L(\bar{x}_L\cos\alpha + \bar{y}_L\sin\alpha) + C_D(\bar{x}_D\sin\alpha - \bar{y}_D\cos\alpha) - \bar{\tilde{C}}_{m_{\text{ac}}}\bar{c}_{\text{mac}} \quad (12)$$

From Eq. (8) and the definition of section aerodynamic center we can write

$$\frac{\partial \bar{\tilde{C}}_{m_{\text{ac}}}}{\partial\alpha} = 0 \quad (13)$$

With the application of Eqs. (1), (2), and (13), the derivatives of Eqs. (9) and (12) with respect to angle of attack yield

$$\bar{x}_{\text{ac}}\frac{\partial}{\partial\alpha}(C_L\cos\alpha + C_D\sin\alpha) + \bar{y}_{\text{ac}}\frac{\partial}{\partial\alpha}(C_L\sin\alpha - C_D\cos\alpha) = \frac{\partial}{\partial\alpha}[C_L(\bar{x}_L\cos\alpha + \bar{y}_L\sin\alpha)] + \frac{\partial}{\partial\alpha}[C_D(\bar{x}_D\sin\alpha - \bar{y}_D\cos\alpha)] = -c_{\text{ref}}\frac{\partial C_{m_0}}{\partial\alpha} \quad (14)$$

The relation between $\bar{x}_{\text{ac}}$ and $\bar{y}_{\text{ac}}$, which is prescribed by Eq. (14), is necessary and sufficient to require the pitching moment about the point $(\bar{x}_{\text{ac}}, \bar{y}_{\text{ac}})$ to have a zero first derivative with respect to angle of attack. However, Eq. (14) does not define a point in the plane of symmetry, rather it defines a line. This line in the wing's plane of symmetry will be referred to here as the neutral axis of the wing, which is formally defined to be the locus of points about which the change in pitching moment with respect to angle of attack is zero, thus satisfying the first criterion in our definition for the aerodynamic center.

In general, Eq. (14) shows that both the slope and the x-axis intercept for the neutral axis of a wing or complete airplane are nonlinear functions of the angle of attack. However, at any given angle of attack the neutral axis is always a straight line. For a small change in angle of attack relative to any given operating condition, the neutral axis will be rotated through a small angle about some point along its length. That point is the aerodynamic center as defined by Eqs. (1) and (2). Every point along the neutral axis satisfies Eq. (1) for the specified angle of attack. However, only one point on the neutral axis also satisfies Eq. (2) for the same angle of attack. Because only the first derivative of $\bar{x}_{\text{ac}}$ and $\bar{y}_{\text{ac}}$ with respect to α is forced to zero, we cannot say that the aerodynamic center is a fixed point, independent of angle of attack. Because there are only 2 degrees of freedom associated with the position of the aerodynamic center, the variation in its position with angle of attack is a matter to be evaluated, not defined. When all nonlinearities are included, the aerodynamic center can be uniquely defined only for small perturbations about any given angle of attack.

Traditional Approximation

Even considering a wing with no dihedral, neglecting drag, and applying the traditional approximation for small angles of attack, Eq. (14) still defines a line in the x–y plane. Using the approximations $C_D \approx 0$, $\cos(\alpha) \approx 1$, and $\sin(\alpha) \approx \alpha$, Eq. (14) reduces to

$$\bar{x}_{\text{ac}}\frac{\partial C_L}{\partial\alpha} + \bar{y}_{\text{ac}}\frac{\partial}{\partial\alpha}(C_L\alpha) = -c_{\text{ref}}\frac{\partial C_{m_0}}{\partial\alpha} \quad (15)$$

For wings with little or no dihedral at small angles of attack, both the lift and the pitching moment are traditionally approximated as linear functions of angle of attack,

$$C_L = C_{L,\alpha}(\alpha - \alpha_{L0}), \qquad C_{L,\alpha,\alpha} = 0, \qquad C_{m0,\alpha,\alpha} = 0 \quad (16)$$

Thus, using Eq. (16) in Eq. (15) and rearranging, we obtain

$$\bar{x}_{\text{ac}} + \bar{y}_{\text{ac}}(2\alpha - \alpha_{L0}) = -c_{\text{ref}}C_{m_0,\alpha}/C_{L,\alpha} \quad (17)$$

This further demonstrates the importance of our refined mathematical definition for the aerodynamic center, which is specified by Eqs. (1) and (2). Even after neglecting drag and applying the small-angle approximation, defining the aerodynamic center according to Eq. (1) yields a line rather than a point. The second criterion given by Eq. (2) is necessary to isolate the aerodynamic center as a point along this line.

For the small-angle approximation in the absence of drag and dihedral effects, the aerodynamic center can be located along the neutral axis by differentiating Eq. (17) with respect to α, subject to Eqs. (2) and (16). This gives

$$\bar{y}_{\text{ac}} = 0 \quad (18)$$

Using this result in Eq. (17) yields the traditional approximation

$$\bar{x}_{\text{ac}} = -c_{\text{ref}}C_{m_0,\alpha}/C_{L,\alpha} \quad (19)$$

In the usual development of Eq. (19), the result given by Eq. (18) is not typically determined mathematically but is simply assumed a priori. Although it may seem obvious that the aerodynamic center of a planar wing should always fall in the plane of the wing, as we shall see, this is not necessarily the case. In extending our analysis for the location of the aerodynamic center to the realm of nonlinear aerodynamics, including the effects of drag and relaxing of the small-angle approximation, we can no longer simply assume that Eq. (18) is valid. The y coordinate of the aerodynamic center must be isolated from the neutral axis defined in Eq. (14) by applying the second criterion of our refined definition for the aerodynamic center, that is, Eq. (2).

Wings with Constant Sweep and Dihedral

Additional insight into the nature of Eq. (14) can be gleaned by considering the special case of a spanwise symmetric wing with constant sweep and constant dihedral in the locus of wing section aerodynamic centers. For wings with this geometry, the axial and normal coordinates of the locus of wing section aerodynamic centers are linear functions of the spanwise coordinate z. For the origin chosen in Fig. 1, we have

$$\tilde{x}_{\text{ac}} = z\tan\Lambda, \qquad \tilde{y}_{\text{ac}} = z\tan\Gamma \quad (20)$$

Using Eq. (20) in Eqs. (6) and (7) gives

$$\bar{x}_L = \bar{z}_L\tan\Lambda, \qquad \bar{y}_L = \bar{z}_L\tan\Gamma, \qquad \bar{z}_L \equiv \frac{2}{C_L S}\int_{z=0}^{b/2}\tilde{C}_L c z\,\mathrm{d}z \quad (21)$$

and

$$\bar{x}_D \equiv \bar{z}_D\tan\Lambda, \qquad \bar{y}_D \equiv \bar{z}_D\tan\Gamma, \qquad \bar{z}_D \equiv \frac{2}{C_D S}\int_{z=0}^{b/2}\tilde{C}_D c z\,\mathrm{d}z \quad (22)$$

With the simplifications introduced by Eqs. (21) and (22), Eq. (14) can be written as

$$\bar{x}_{\text{ac}}\frac{\partial}{\partial\alpha}(C_L\cos\alpha + C_D\sin\alpha) + \bar{y}_{\text{ac}}\frac{\partial}{\partial\alpha}(C_L\sin\alpha - C_D\cos\alpha)$$
$$= \tan\Lambda\frac{\partial}{\partial\alpha}(\bar{z}_L C_L\cos\alpha + \bar{z}_D C_D\sin\alpha)$$
$$+ \tan\Gamma\frac{\partial}{\partial\alpha}(\bar{z}_L C_L\sin\alpha - \bar{z}_D C_D\cos\alpha) \tag{23}$$

From this relation we see that, for wings with constant sweep and constant dihedral, the wing's neutral axis can be determined as a function of angle of attack from knowledge of the sweep and dihedral angles, the lift and drag coefficients, and the spanwise positions of the semispan centers of lift and drag. In general, C_L, C_D, $\bar{z}_L$, and $\bar{z}_D$ all vary with angle of attack. Furthermore, $\bar{z}_L$ and $\bar{z}_D$ are not necessarily coincident.

General Relations for Aerodynamic Center

Equation (14) defines the neutral axis of a wing in terms of the lift and drag coefficients for the wing and the locations of the aerodynamic centers of lift and drag. Because an analytical solution does not exist for the spanwise distributions of lift and drag acting on a wing of arbitrary geometry, the position of the aerodynamic center must be evaluated numerically or experimentally for wings with arbitrary sweep and/or dihedral. Although Eq. (14) provides valuable insight into how the aerodynamic center is affected by lift and drag, for experimental or numerical evaluation of the aerodynamic center it is more convenient to write Eq. (14) in terms of the axial and normal force coefficients,

$$C_A = C_D\cos\alpha - C_L\sin\alpha \tag{24}$$

$$C_N = C_L\cos\alpha + C_D\sin\alpha \tag{25}$$

Applying Eqs. (24) and (25) to Eqs. (11) and (14) yields

$$C_{m_0}c_{\text{ref}} = C_{m_{\text{ac}}}c_{\text{ref}} - \bar{x}_{\text{ac}}C_N + \bar{y}_{\text{ac}}C_A \tag{26}$$

$$\bar{x}_{\text{ac}}C_{N,\alpha} - \bar{y}_{\text{ac}}C_{A,\alpha} = -C_{m_0,\alpha}c_{\text{ref}} \tag{27}$$

Equation (27) defines the wing's neutral axis at some arbitrary angle of attack α. Every point along this neutral axis satisfies the first criterion in our refined definition for the aerodynamic center, which is given by Eq. (1). The aerodynamic center of the wing can be isolated from the neutral axis by differentiating Eq. (27) with respect to angle of attack and applying the second criterion in our definition for the aerodynamic center, which is given by Eq. (2). This gives

$$\bar{x}_{\text{ac}}C_{N,\alpha,\alpha} - \bar{y}_{\text{ac}}C_{A,\alpha,\alpha} = -C_{m_0,\alpha,\alpha}c_{\text{ref}} \tag{28}$$

The aerodynamic center of the wing is the only point common to the two lines, which are defined by Eqs. (27) and (28). Solving Eqs. (27) and (28) for the position of the aerodynamic center and using the result in Eq. (26) yields

$$\bar{x}_{\text{ac}} = \frac{C_{A,\alpha}C_{m_0,\alpha,\alpha} - C_{m_0,\alpha}C_{A,\alpha,\alpha}}{C_{N,\alpha}C_{A,\alpha,\alpha} - C_{A,\alpha}C_{N,\alpha,\alpha}}c_{\text{ref}} \tag{29}$$

$$\bar{y}_{\text{ac}} = \frac{C_{N,\alpha}C_{m_0,\alpha,\alpha} - C_{m_0,\alpha}C_{N,\alpha,\alpha}}{C_{N,\alpha}C_{A,\alpha,\alpha} - C_{A,\alpha}C_{N,\alpha,\alpha}}c_{\text{ref}} \tag{30}$$

$$C_{m_{\text{ac}}}c_{\text{ref}} = C_{m_0}c_{\text{ref}} + \bar{x}_{\text{ac}}C_N - \bar{y}_{\text{ac}}C_A \tag{31}$$

Because the choice of coordinate system origin in these relations is arbitrary, Eqs. (29–31) can be used to determine the position of the aerodynamic center and the pitching moment about this aerodynamic center from analytical results, numerical computations, or experimental measurements for the resultant aerodynamic force components, pitching moment, and their first and second derivatives, obtained relative to any point in the x–y plane.

For the traditional approximation obtained using linearized aerodynamics and neglecting the effects of drag, Eqs. (24) and (25) are approximated as

$$C_A \cong -C_{L,\alpha}(\alpha - \alpha_{L0})\alpha, \qquad C_N \cong C_{L,\alpha}(\alpha - \alpha_{L0}) \tag{32}$$

which yields

$$C_{A,\alpha} \cong -C_{L,\alpha}(2\alpha - \alpha_{L0}), \qquad C_{N,\alpha} \cong C_{L,\alpha} \tag{33}$$

Because the lift and pitching moment coefficients are assumed to be linear functions of the angle of attack, this traditional approximation applied to the second derivative terms in Eqs. (29) and (30) results in

$$C_{A,\alpha,\alpha} \cong -2C_{L,\alpha}, \qquad C_{N,\alpha,\alpha} \cong 0, \qquad C_{m0,\alpha,\alpha} \cong 0 \tag{34}$$

Using Eqs. (33) and (34) in Eqs. (29) and (30) produces the traditional approximation

$$\bar{x}_{\text{ac}} \cong -\frac{C_{m_0,\alpha}}{C_{L,\alpha}}c_{\text{ref}}, \qquad \bar{y}_{\text{ac}} \cong 0 \tag{35}$$

The error introduced by neglecting drag and applying the traditional small-angle approximation can be evaluated by simply including drag in Eqs. (29) and (30) and comparing the result with Eq. (35).

Planar Wing Example Using Computational Fluid Dynamics

To demonstrate how the aerodynamic and trigonometric nonlinearities affect the position of the aerodynamic center of a swept wing, we consider a wing of aspect ratio 6.0 and taper ratio 0.5 with a constant quarter-chord sweep angle of 30 deg. To isolate the effects of the nonlinearities and sweep from other effects, the wing is constructed with a NACA 0012 airfoil section and has no twist or dihedral. This wing geometry was analyzed using computational fluid dynamics (CFD) to determine the position of the aerodynamic center as a function of angle of attack from -5 to $+18$ deg.

All calculations were performed using version 6 of the computational fluid dynamics code CFL3D [5]. This is a structured-grid, multizone code that solves the three-dimensional, time-dependent, Reynolds-averaged, Navier–Stokes equations using an upwind finite volume formulation. The code uses a third-order upwind-biased interpolation scheme for the convective and pressure terms. Local time stepping, mesh sequencing, and low-Mach-number preconditioning were also used. The Spalart–Allmaras turbulence model [6] was used for all computations and all results were obtained for a freestream Mach number of 0.10 and a freestream Reynolds number of 1.0×10^6.

All computations were performed using C-O grids generated about one semispan of the wing. Inflow/outflow boundary conditions were specified on the far-field planes and symmetry conditions were used along the bounding plane at the wing root. No-slip boundary conditions were specified on the wing surface. Nodes were clustered in the normal direction near the wing surface and in the spanwise direction near the wingtip. Nodes were also clustered in the wake region aft of the wingtip to provide improved resolution of the wingtip vortex. To keep the wingtip vortex confined to the wake region where nodes were clustered, a different grid was generated for each angle of attack studied. As the angle of attack was changed, the wing was rotated relative to the grid so that the freestream velocity vector was closely aligned with the x axis of the grid and the region of wake clustering. For a more detailed description of the grids used for the present study, see Alley et al. [7].

To ensure that the solutions were grid resolved for each operating condition considered, mesh sequencing was employed in the solution procedure using coarse, intermediate, and fine grids, which contained 383,377; 2,989,305; and 23,606,737 nodes, respectively. The fine grids had 121 spanwise sections with 385 nodes spaced around the circumference of each wing section. An additional

208 streamwise nodes were included in the trailing wake for each spanwise section. A total of 329 radial layers were used to create these $593 \times 329 \times 121$ C-O grids. The radial layers were clustered in the region close to the wing so that the normal grid spacing at the wing surface was reduced to 7.5×10^{-7} chord lengths. In all cases, the average y^+ value for the surface boundary elements of the fine grid was less than 0.1. The intermediate grids were obtained within CFL3D from the fine grids by deleting alternate points in each direction. The coarse grids were derived from the intermediate grids in a similar manner. Using converged results from the coarse, intermediate, and fine grids, an improved estimate for the grid resolved solution was obtained using the Richardson extrapolation [8,9]. To implement the extrapolation, the procedure described by Phillips et al. [10] was used.

Results obtained from these C-O grids for the wing lift, drag, and pitching moment coefficient about the origin of the coordinate system in Fig. 1 are shown in Figs. 2–4, respectively. The y^+ values given in these figures are the maximum average values for any angle of attack, which occurred near the largest angle of attack. Using the Richardson extrapolations shown in these figures, the derivatives in Eqs. (29) and (30) were evaluated numerically using fourth-order interpolation and the results shown in Fig. 5 were obtained from Eqs. (29) and (30).

For the results presented in Figs. 2–5, the arbitrary reference length used for computing the wing pitching moment coefficient was specified to be the geometric mean chord length, S/b. The 24 aerodynamic centers shown in Fig. 5 are, from top to bottom, for angles of attack from -5 to $+18$ deg in 1-deg increments. For comparison, the wing's neutral axis is also shown in Fig. 5, for angles of attack of $-5, 0, 5, 10$, and 15 deg. Notice that the neutral axis at any angle of attack passes through the aerodynamic center for the same angle of attack and is tangent to the curve defined by the locus of aerodynamic centers.

At zero angle of attack, the wing's neutral axis is vertical and the aerodynamic center of this wing is located at the coordinates $\bar{x}_{\text{ac}}/c_{\text{ref}} = 0.7311$ and $\bar{y}_{\text{ac}}/c_{\text{ref}} = 0.0000$, which agrees very closely with the traditional approximation given by Eq. (35). As the angle of attack is increased from zero, the wing's neutral axis is rotated counterclockwise and the aerodynamic center is moved slightly aft and below the plane of the wing. To gain some insight into the physics behind this phenomenon, we recognize that at zero angle of attack the position of the aerodynamic center is dominated by lift. Thus, the aerodynamic center at zero angle of attack is nearly coincident with the center of additional lift. Because this wing has no twist, the center of additional lift is also the center of total lift [11]. For this wing geometry the aerodynamic center of lift is located at $\bar{x}_L/c_{\text{ref}} = 0.7326$ and $\bar{y}_L/c_{\text{ref}} = 0.0000$.

Because this wing has no camber or twist, the drag at zero angle of attack is all parasitic drag and the section drag coefficient is nearly uniform over the wingspan. Thus, the aerodynamic center of drag at

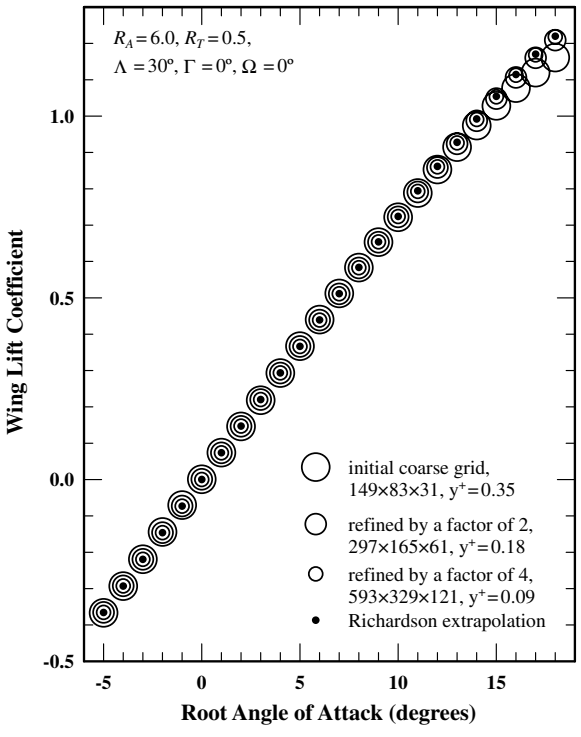

Fig. 2 Wing lift coefficient vs angle of attack as predicted from CFD.

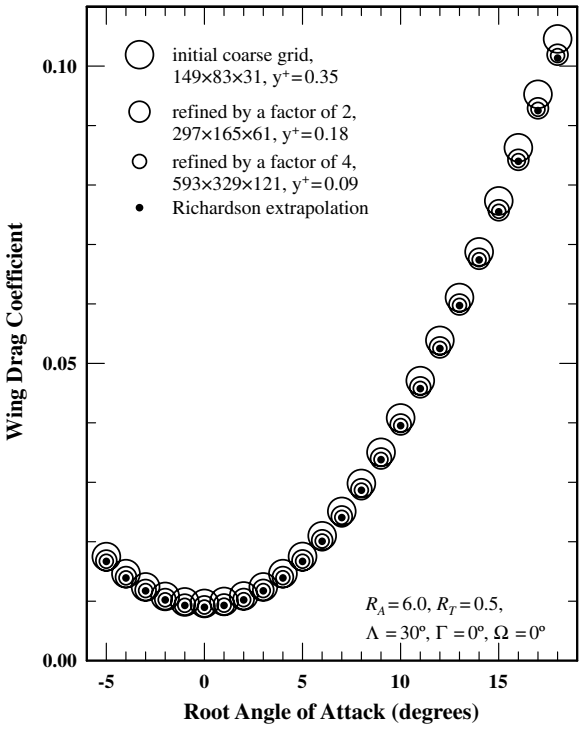

Fig. 3 Wing drag coefficient vs angle of attack as predicted from CFD.

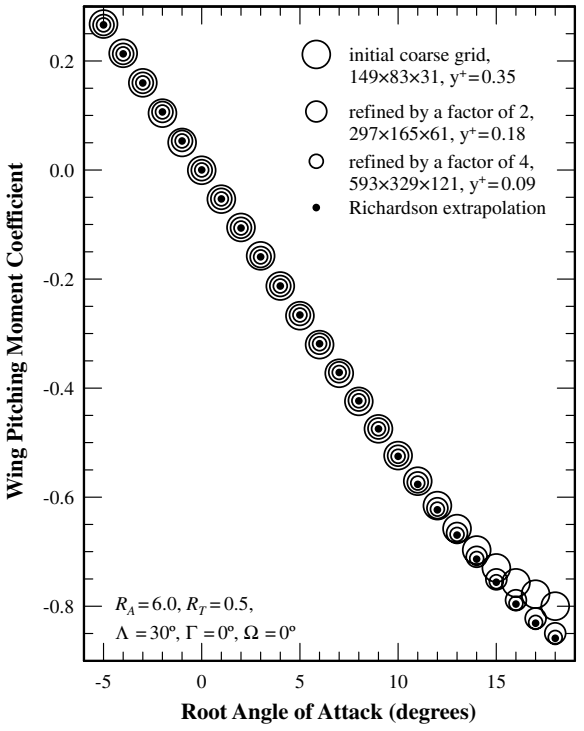

Fig. 4 Wing pitching moment coefficient about the origin vs angle of attack as predicted from CFD.

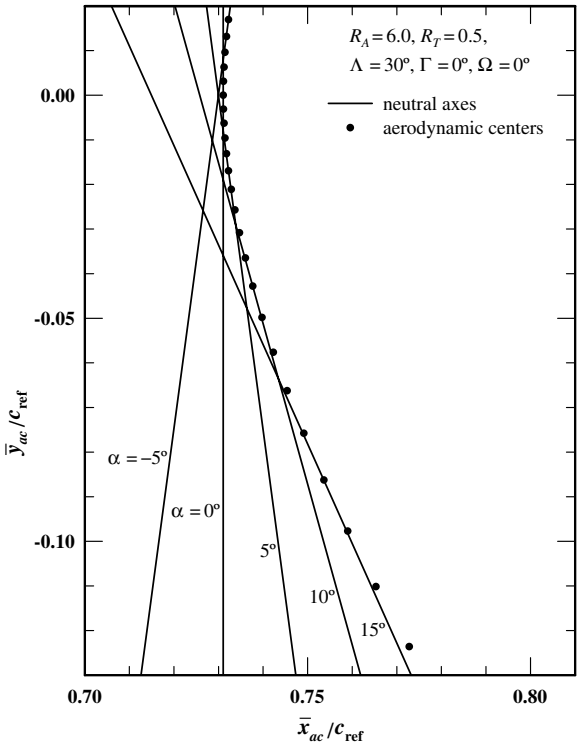

Fig. 5 Wing aerodynamic centers and neutral axes as predicted from CFD.

zero angle of attack should be located very near the aerodynamic center of the centroidal chord, which for this particular wing is located at $x/c_{\text{ref}} = 0.7698$ and $y/c_{\text{ref}} = 0.0000$ as shown in Fig. 6.

With this line of reasoning, we see that the wing's aerodynamic center of drag is slightly aft of the aerodynamic center of lift at zero angle of attack. Because this wing has no twist, the center of total lift does not move significantly with small changes in angle of attack [12]. However, as the angle of attack is increased, induced drag becomes an increasing fraction of the total drag. Because induced drag is greatest near the wingtips, increasing the angle of attack for this swept wing moves the aerodynamic center of drag outboard and aft. Thus, we see that for this wing geometry at angles of attack below stall, the aerodynamic center of drag is always aft of the aerodynamic center of lift. This requires that the center of aerodynamic force, which is defined in Fig. 7, is always below the plane of the wing at positive angles of attack. Although the aerodynamic center of the wing does not necessarily fall at the center of aerodynamic force, we should not be too surprised to learn from the CFD results that the aerodynamic center of this wing also falls below the plane of the wing at positive angles of attack below stall.

From Fig. 5, we see that the aerodynamic center moves aft by about 4% of the mean chord and down by more than 12% of the mean chord, as the angle of attack changes from zero to somewhat below maximum lift. This movement is significant in view of the fact that

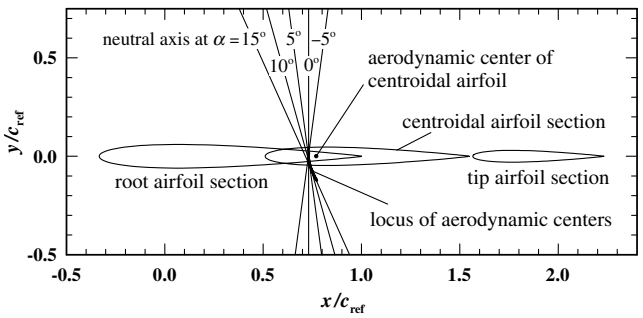

Fig. 6 Locus of aerodynamic centers and neutral axes compared with the wing geometry.

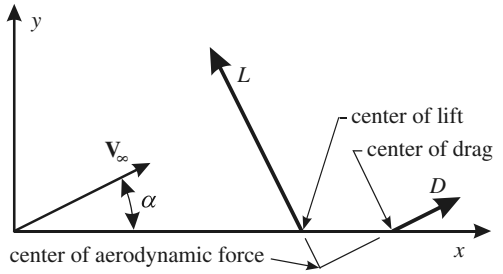

Fig. 7 Center of aerodynamic force, defined here to be the intersection of the wing lift and drag vectors.

the design static margin is often on the order of 5% of the mean chord. It is significant to note that the aft movement of the aerodynamic center, which is shown in Figs. 5 and 6, is stabilizing at angles of attack below stall, because the normal force increases with increasing angle of attack. However, the vertical movement of the aerodynamic center shown in these figures also affects pitch stability and the nature of this effect may not be quite so obvious. To examine the net effect of this aerodynamic center movement on pitch stability, consider the variations in the aerodynamic force coefficients with angle of attack for the planar wing in this example, which are shown in Fig. 8. From Eq. (26), the pitch-stability derivative about the center of gravity can be written as

$$C_{m,\alpha} = -\frac{\bar{x}_{\text{ac}} - x_{\text{c.g.}}}{c_{\text{ref}}} C_{N,\alpha} + \frac{\bar{y}_{\text{ac}} - y_{\text{c.g.}}}{c_{\text{ref}}} C_{A,\alpha} \tag{36}$$

where $x_{\text{c.g.}}$ and $y_{\text{c.g.}}$ are the x and y coordinates of the center of gravity. From Fig. 8, we see that, at angles of attack below stall, $C_{N,\alpha}$ is always positive. Thus, the first term on the right-hand side of Eq. (36) confirms the well-known fact that moving the aerodynamic center of a wing aft (i.e., increasing $\bar{x}_{\text{ac}}$) is stabilizing. On the other hand, Fig. 8 also shows that, at positive angles of attack below stall, $C_{A,\alpha}$ is negative. Thus, the second term on the right-hand side of Eq. (36) shows that moving the aerodynamic center down (i.e., decreasing $\bar{y}_{\text{ac}}$) is destabilizing at positive angles of attack below stall. When the angle of attack is small, the effect of the aft movement of the aerodynamic center with increasing angle of attack tends to cancel the effect of the downward movement and the net effect is slight. At higher angles of attack the net effect is destabilizing. This is demonstrated in Fig. 9, which shows the pitching moment about the point $x/c_{\text{ref}} = 0.6811$ and $y/c_{\text{ref}} = 0.0000$. This point is forward of the aerodynamic center at $\alpha = 0$ by 5% of the mean chord. At zero angle of attack, the pitch-stability derivative taken from Fig. 9 is approximately -0.128. However, as the angle of attack approaches maximum lift, the movement of the aerodynamic center changes the pitch-stability derivative to about -0.047. This represents a

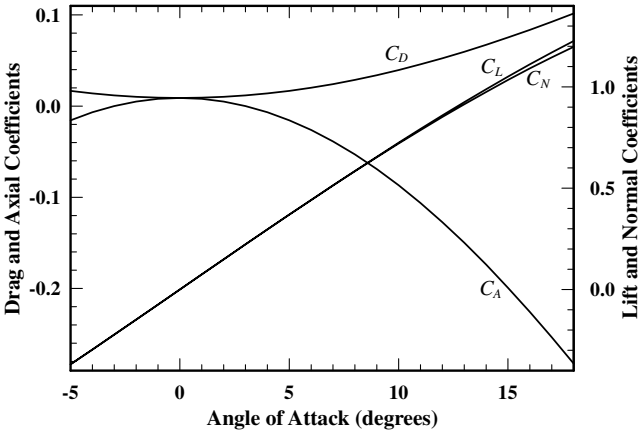

Fig. 8 Aerodynamic force coefficients predicted from computational fluid dynamics.

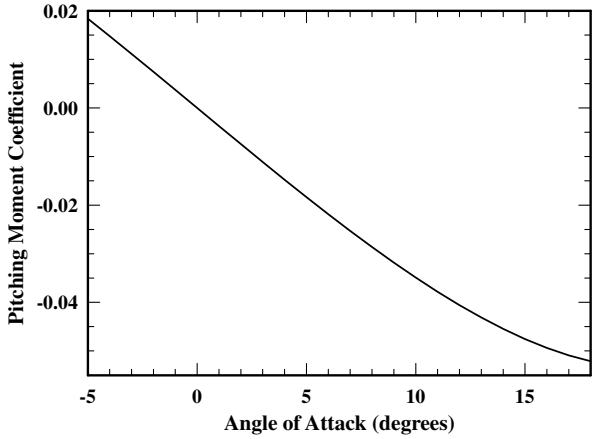

Fig. 9 Pitching moment coefficient about a point forward of the zero-angle-of-attack aerodynamic center by 5% of the mean chord.

reduction in pitch stability of more than 63%, which is clearly significant.

Closed-Form Approximation for a System of Two Lifting Surfaces

From the previous example we have seen that, when combined with wing sweep, the nonlinearities in the trigonometric functions and the aerodynamic force and moment components can have a significant effect on the vertical position of the aerodynamic center of a single lifting surface. Furthermore, when the aerodynamic center of an airplane is vertically offset from the center of gravity (c.g.), these same nonlinearities can have an important effect on aircraft stability. A substantial nonlinear variation in the pitching moment with respect to angle of attack will typically occur whenever the c.g. is not in close vertical alignment with the aerodynamic center of an airplane. When the aerodynamic center is substantially above the c.g., an aircraft can become "unstable" in response to large negative disturbances in angle of attack, even though the aircraft is "mathematically stable" with respect to infinitesimal pitch disturbances. For this and other reasons, it can be important to know both the horizontal and vertical locations of the aerodynamic center of an aircraft as determined with the nonlinearities included.

To gain additional insight into how the nonlinearities affect the pitch-stability derivative for a complete airplane, we shall consider a system of two lifting surfaces, which is composed of a main wing and a horizontal control surface. A schematic of the force and moment components acting on such a system is shown in Fig. 10. Here the position and orientation of each lifting surface is described relative to an arbitrary coordinate system, the origin of which may or may not be located at the aircraft's center of gravity.

The most serious approximation associated with the analysis to be presented in this section is that we shall approximate the vortex interactions between the two lifting surfaces by simply using an average downwash angle for each surface, which is assumed proportional to the lift developed on the other surface. In reality, the downwash or upwash (negative downwash) can vary substantially over the span of each lifting surface. For example, the downwash induced on the main wing by a forward canard varies from positive near the wing root to negative in the regions outboard of the tip vortices shed from the canard. Nevertheless, reasonably accurate results can be obtained from the approximation used here and it yields important insight into how and why the nonlinearities in the trigonometric functions and the aerodynamic force and moment components affect aircraft stability.

In Fig. 10, the horizontal control surface was drawn in the configuration of an aft tail. However, the results of the following analysis can be applied to either an aft tail or a forward canard. The canard is distinguished from the aft tail only by the relative positions x_w and x_h, and the signs of ε_w and ε_h. For an aft tail, x_h is greater than x_w, whereas for the canard, x_h is less than x_w. A lifting wing induces downwash on an aft tail, and when the tail is producing positive lift, it induces upwash on the wing. Thus, for the aft tail configuration, ε_h has the same sign as the lift on the wing and ε_w has the opposite sign from that of the lift on the tail. Conversely, for the wing–canard configuration, ε_w has the same sign as the lift on the canard and ε_h takes the sign opposite to that for the lift on the wing. Therefore, we need not make any distinction between the wing–tail and wing–canard configurations. The numerical values used in the formulation will take care of the differences.

From Fig. 10 the net axial force coefficient for this system of lifting surfaces is

$$C_A = C_{D_w}\cos(\alpha-\varepsilon_w) - C_{L_w}\sin(\alpha-\varepsilon_w) + \frac{S_h}{S_w}[C_{D_h}\cos(\alpha-\varepsilon_h) - C_{L_h}\sin(\alpha-\varepsilon_h)] \tag{37}$$

and the net normal force coefficient is

$$C_N = C_{L_w}\cos(\alpha-\varepsilon_w) + C_{D_w}\sin(\alpha-\varepsilon_w) + \frac{S_h}{S_w}[C_{L_h}\cos(\alpha-\varepsilon_h) + C_{D_h}\sin(\alpha-\varepsilon_h)] \tag{38}$$

Similarly, the net pitching moment coefficient about the coordinate system origin can be written

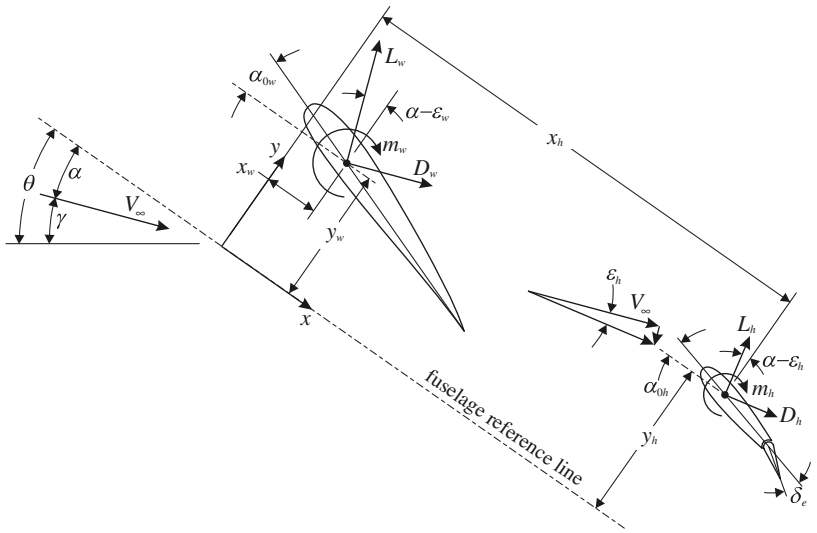

Fig. 10 Force and moment components acting on a wing combined with a horizontal control surface.

$$C_{m_0}c_{\text{ref}} = C_{m_w}\bar{c}_w + \frac{S_h}{S_w}C_{m_h}\bar{c}_h - (x_w C_{L_w} - y_w C_{D_w})\cos(\alpha-\varepsilon_w)$$
$$-(x_w C_{D_w} + y_w C_{L_w})\sin(\alpha-\varepsilon_w) - \frac{S_h}{S_w}(x_h C_{L_h} - y_h C_{D_h})\cos(\alpha-\varepsilon_h)$$
$$-\frac{S_h}{S_w}(x_h C_{D_h} + y_h C_{L_h})\sin(\alpha-\varepsilon_h) \tag{39}$$

where the pitching moment coefficient about the aerodynamic center of the horizontal control surface depends on elevator deflection. In the absence of stall, the lift coefficients for the main wing and the horizontal control surface can be closely approximated as linear functions of angle of attack

$$C_{L_w} = C_{L_{w,\alpha}}(\alpha + \alpha_{0w} - \alpha_{L0w} - \varepsilon_w) \tag{40}$$

$$C_{L_h} = C_{L_{h,\alpha}}(\alpha + \alpha_{0h} - \alpha_{L0h} - \varepsilon_h) \tag{41}$$

where the zero-lift angle of attack for the horizontal control surface depends on elevator deflection. Similarly, the drag coefficients for the wing and horizontal control surface can be written as parabolic functions of lift coefficient

$$C_{D_w} = C_{D_{0w}} + C_{D_0,L_w}C_{L_w} + \frac{C_{L_w}^2}{\pi e_w R_{A_w}} \tag{42}$$

$$C_{D_h} = C_{D_{0h}} + C_{D_0,L_h}C_{L_h} + \frac{C_{L_h}^2}{\pi e_h R_{A_h}} \tag{43}$$

To close this formulation we now approximate the average downwash angle for each lifting surface as being linearly proportional to the lift developed on the other surface

$$\varepsilon_w = C_{\varepsilon w}C_{L_h} \tag{44}$$

$$\varepsilon_h = C_{\varepsilon h}C_{L_w} \tag{45}$$

The proportionality constants $C_{\varepsilon w}$ and $C_{\varepsilon h}$ could be estimated from the vortex model presented by McCormick [13] and Phillips [14]. The signs of these constants depend on the aircraft configuration. For the wing–tail configuration, $C_{\varepsilon w}$ is negative and $C_{\varepsilon h}$ is positive. For the wing–canard configuration, $C_{\varepsilon w}$ is positive and $C_{\varepsilon h}$ is negative.

Using Eqs. (44) and (45) in Eqs. (40) and (41) produces the coupled system

$$\begin{bmatrix} 1 & C_{\varepsilon w}C_{L_{w,\alpha}} \\ C_{\varepsilon h}C_{L_{h,\alpha}} & 1 \end{bmatrix}\begin{Bmatrix} C_{L_w} \\ C_{L_h} \end{Bmatrix} = \begin{Bmatrix} C_{L_{w,\alpha}}(\alpha + \alpha_{0w} - \alpha_{L0w}) \\ C_{L_{h,\alpha}}(\alpha + \alpha_{0h} - \alpha_{L0h}) \end{Bmatrix} \equiv \begin{Bmatrix} C_{L_{w0}} \\ C_{L_{h0}} \end{Bmatrix} \tag{46}$$

which is readily solved to yield

$$\begin{Bmatrix} C_{L_w} \\ C_{L_h} \end{Bmatrix} = \begin{Bmatrix} \dfrac{C_{L_{w0}} - (C_{\varepsilon w}C_{L_{w,\alpha}})C_{L_{h0}}}{1-(C_{\varepsilon w}C_{L_{w,\alpha}})(C_{\varepsilon h}C_{L_{h,\alpha}})} \\ \dfrac{C_{L_{h0}} - (C_{\varepsilon h}C_{L_{h,\alpha}})C_{L_{w0}}}{1-(C_{\varepsilon w}C_{L_{w,\alpha}})(C_{\varepsilon h}C_{L_{h,\alpha}})} \end{Bmatrix} \tag{47}$$

For a given angle of attack, the individual lift coefficients can be evaluated from Eq. (47) and the result can be used in Eqs. (42–45) to evaluate the individual drag coefficients and the downwash angles. With these results, the axial and normal force coefficients as well as the pitching moment coefficient for the system can be evaluated from Eqs. (37–39). Using the first and second derivatives of Eqs. (37–39), the position of the aerodynamic center is readily evaluated from Eqs. (29) and (30).

Traditional Approximation

The conventional linearized formulation can be obtained from Eqs. (37–39) by neglecting drag, applying the small-angle approximation, and assuming that only the normal force contributes to the pitching moment. This gives

$$C_A = -(C_w + C_h)\alpha \tag{48}$$

$$C_N = C_w + C_h \tag{49}$$

$$C_{m_0}c_{\text{ref}} = C_{m_w}\bar{c}_w + \frac{S_h}{S_w}C_{m_h}\bar{c}_h - x_w C_w - x_h C_h \tag{50}$$

where after applying Eq. (47)

$$C_w = \frac{C_{L_w0} - (C_{\varepsilon w}C_{L_{w,\alpha}})C_{L_h0}}{1-(C_{\varepsilon w}C_{L_{w,\alpha}})(C_{\varepsilon h}C_{L_{h,\alpha}})} \tag{51}$$

$$C_h = \frac{S_h}{S_w}\frac{C_{L_h0} - (C_{\varepsilon h}C_{L_{h,\alpha}})C_{L_h0}}{1-(C_{\varepsilon w}C_{L_{w,\alpha}})(C_{\varepsilon h}C_{L_{h,\alpha}})} \tag{52}$$

From the definitions in Eq. (46), the first and second derivatives of Eqs. (51) and (52) with respect to α yield

$$C_{w,\alpha} = \frac{C_{L_{w,\alpha}}(1 - C_{\varepsilon w}C_{L_{h,\alpha}})}{1-(C_{\varepsilon w}C_{L_{w,\alpha}})(C_{\varepsilon h}C_{L_{h,\alpha}})} \tag{53}$$

$$C_{h,\alpha} = \frac{S_h}{S_w}\frac{C_{L_{h,\alpha}}(1 - C_{\varepsilon h}C_{L_{w,\alpha}})}{1-(C_{\varepsilon w}C_{L_{w,\alpha}})(C_{\varepsilon h}C_{L_{h,\alpha}})} \tag{54}$$

$$C_{w,\alpha,\alpha} = C_{h,\alpha,\alpha} = 0 \tag{55}$$

Thus, differentiating Eqs. (48–50) twice with respect to α results in

$$C_{A,\alpha} = -(C_{w,\alpha} + C_{h,\alpha})\alpha - (C_w + C_h) \tag{56}$$

$$C_{N,\alpha} = C_{w,\alpha} + C_{h,\alpha} \tag{57}$$

$$C_{m_0,\alpha}c_{\text{ref}} = -x_w C_{w,\alpha} - x_h C_{h,\alpha} \tag{58}$$

$$C_{A,\alpha,\alpha} = -2(C_{w,\alpha} + C_{h,\alpha}) \tag{59}$$

$$C_{N,\alpha,\alpha} = C_{m_0,\alpha,\alpha}c_{\text{ref}} = 0 \tag{60}$$

Applying Eqs. (56–60) to Eqs. (29) and (30) gives the traditional approximation,

$$\bar{x}_{\text{ac}} = \frac{x_w C_{w,\alpha} + x_h C_{h,\alpha}}{C_{w,\alpha} + C_{h,\alpha}}, \qquad \bar{y}_{\text{ac}} = 0 \tag{61}$$

In the usual development of Eq. (61), the y coordinate of the aerodynamic center is not determined mathematically but is either assumed a priori or simply ignored.

Nonlinear Zero-Drag Approximation

To compare the relative effects of neglecting drag and applying the small-angle approximation, we shall now examine the approximation obtained by neglecting only the drag without applying the small-angle approximation. Neglecting all forms of drag, including the drag induced on one lifting surface by the other, Eqs. (37–39) become

$$C_A = -(C_w + C_h)\sin\alpha \tag{62}$$

$$C_N = (C_w + C_h)\cos\alpha \tag{63}$$

$$C_{m_0}c_{\text{ref}} = C_{m_w}\bar{c}_w + \frac{S_h}{S_w}C_{m_h}\bar{c}_h - (x_wC_w + x_hC_h)\cos\alpha - (y_wC_w + y_hC_h)\sin\alpha \tag{64}$$

and the first and second derivatives of Eqs. (62–64) with respect to α yield

$$C_{A,\alpha} = -(C_{w,\alpha} + C_{h,\alpha})\sin\alpha - (C_w + C_h)\cos\alpha \tag{65}$$

$$C_{N,\alpha} = (C_{w,\alpha} + C_{h,\alpha})\cos\alpha - (C_w + C_h)\sin\alpha \tag{66}$$

$$C_{m_0,\alpha}c_{\text{ref}} = -(x_wC_{w,\alpha} + x_hC_{h,\alpha} + y_wC_w + y_hC_h)\cos\alpha + (x_wC_w + x_hC_h - y_wC_{w,\alpha} - y_hC_{h,\alpha})\sin\alpha \tag{67}$$

$$C_{A,\alpha,\alpha} = -2(C_{w,\alpha} + C_{h,\alpha})\cos\alpha + (C_w + C_h)\sin\alpha \tag{68}$$

$$C_{N,\alpha,\alpha} = -2(C_{w,\alpha} + C_{h,\alpha})\sin\alpha - (C_w + C_h)\cos\alpha \tag{69}$$

$$C_{m_0,\alpha,\alpha}c_{\text{ref}} = (2x_wC_{w,\alpha} + 2x_hC_{h,\alpha} + y_wC_w + y_hC_h)\sin\alpha + (x_wC_w + x_hC_h - 2y_wC_{w,\alpha} - 2y_hC_{h,\alpha})\cos\alpha \tag{70}$$

Applying Eqs. (65–70) to Eqs. (29) and (30) yields a zero-drag approximation for the aerodynamic center.

Using Eqs. (37–47) combined with Eqs. (29) and (30) allows us to predict the position of the aerodynamic center, including the effects of the nonlinearities in the trigonometric functions and the drag. A more approximate estimate for the location of the aerodynamic center can be found by neglecting drag but including the trigonometric nonlinearities, which results in the formulation given by Eqs. (62–70) combined with Eqs. (29) and (30). For aircraft without highly swept wings, the results predicted from these two formulations are nearly equivalent. Furthermore, the x coordinate of the aerodynamic center as predicted from either of these two models does not differ greatly from that predicted from the traditional approximation given by Eq. (61). The problem with the traditional small-angle approximation is not that it provides an unreasonable estimate for the axial position of the aerodynamic center. The problem is that it provides no estimate for the vertical position.

Improved Linear Approximation

An improved small-angle formulation, which does provide an estimate for the y coordinate of the aerodynamic center, can be obtained by applying the small-angle approximation to Eqs. (62–64). This gives

$$C_A = -(C_w + C_h)\alpha \tag{71}$$

$$C_N = C_w + C_h \tag{72}$$

$$C_{m_0}c_{\text{ref}} = C_{m_w}\bar{c}_w + \frac{S_h}{S_w}C_{m_h}\bar{c}_h - x_wC_w - x_hC_h - (y_wC_w + y_hC_h)\alpha \tag{73}$$

$$C_{A,\alpha} = -(C_{w,\alpha} + C_{h,\alpha})\alpha - C_w - C_h \tag{74}$$

$$C_{N,\alpha} = C_{w,\alpha} + C_{h,\alpha} \tag{75}$$

$$C_{m_0,\alpha}c_{\text{ref}} = -x_wC_{w,\alpha} - x_hC_{h,\alpha} - (y_wC_{w,\alpha} + y_hC_{h,\alpha})\alpha - y_wC_w - y_hC_h \tag{76}$$

$$C_{A,\alpha,\alpha} = -2(C_{w,\alpha} + C_{h,\alpha}) \tag{77}$$

$$C_{N,\alpha,\alpha} = 0 \tag{78}$$

$$C_{m_0,\alpha,\alpha}c_{\text{ref}} = -2(y_wC_{w,\alpha} + y_hC_{h,\alpha}) \tag{79}$$

Applying Eqs. (74–79) to Eqs. (29) and (30) results in

$$\bar{x}_{\text{ac}} = \frac{x_wC_{w,\alpha} + x_hC_{h,\alpha}}{C_{w,\alpha} + C_{h,\alpha}} + \frac{(y_h - y_w)[C_{w,\alpha}C_{h0} - C_{h,\alpha}C_{w0}]}{(C_{w,\alpha} + C_{h,\alpha})^2} \tag{80}$$

$$\bar{y}_{\text{ac}} = \frac{y_wC_{w,\alpha} + y_hC_{h,\alpha}}{C_{w,\alpha} + C_{h,\alpha}} \tag{81}$$

where C_{w0} and C_{h0} are the zero-angle-of-attack contributions to the net lift coefficient from the main wing and the horizontal control surface, respectively,

$$C_{w0} = \frac{C_{L_w,\alpha}}{1 - (C_{\varepsilon w}C_{L_w,\alpha})(C_{\varepsilon h}C_{L_h,\alpha})} \times [(\alpha_{0w} - \alpha_{L0w}) - C_{\varepsilon w}C_{L_h,\alpha}(\alpha_{0h} - \alpha_{L0h})] \tag{82}$$

$$C_{h0} = \frac{S_h}{S_w}\frac{C_{L_h,\alpha}}{1 - (C_{\varepsilon w}C_{L_w,\alpha})(C_{\varepsilon h}C_{L_h,\alpha})} \times [(\alpha_{0h} - \alpha_{L0h}) - C_{\varepsilon h}C_{L_w,\alpha}(\alpha_{0w} - \alpha_{L0w})] \tag{83}$$

Note that, if the aerodynamic centers of the wing and horizontal control surface have the same vertical coordinate, Eq. (80) gives the same axial coordinate as Eq. (61). Otherwise, Eqs. (80) and (81) predict a first-order correction to the traditional approximation for both the axial and vertical coordinates of the aerodynamic center.

Wing–Canard Example

The following example illustrates the criticality of the vertical location of the aerodynamic center. Unswept lifting surfaces were chosen for this example specifically to minimize the movement of the aerodynamic center with angle of attack. The demonstrated effect will be more pronounced for those geometries with substantial sweep and larger consequent vertical variation in the position of the aerodynamic center.

To demonstrate how nonlinearities can affect the position of the aerodynamic center of an aircraft, we consider a wing–canard configuration. The wing and canard are geometrically similar, having a linear taper with aspect ratios of 6.05 and taper ratios of 0.40. The wing and canard have the same airfoil sections with no twist and no quarter-chord sweep or dihedral. The main wing has a planform area of 180 ft^2 with its quarter chord located 3.00 ft aft and 4.00 ft above the fuselage reference origin. The canard has a planform area of 36 ft^2 and its quarter chord is vertically aligned with and 12.00 ft forward of the fuselage reference origin. The zero-lift angle of attack for the airfoil section used for both the wing and the canard is −2.20 deg. The wing has a positive mounting angle relative to the fuselage reference line of 1.80 deg, and the canard is mounted at 4.00 deg to the fuselage reference line. For these computations we shall use the constant airfoil section coefficients $\tilde{C}_{L,\alpha} = 5.87$, $\tilde{C}_D = 0.008$, and $\tilde{C}_{m_{\text{ac}}} = -0.053$ for both the wing and the canard. As obtained from lifting-line theory, we also use $C_{L_w,\alpha} = C_{L_h,\alpha} = 4.44$, $C_{D_0,L_w} = C_{D_0,L_h} = 0.00$, $e_w = e_h = 0.99$, $C_{\varepsilon w} = 0.017$, and $C_{\varepsilon h} = -0.012$.

Using Eqs. (37–39), the results presented in Fig. 11 were obtained. The canard lift coefficient plotted in this figure is based on the planform area of the canard. All other coefficients shown in Fig. 11 were computed using the planform area of the main wing as the reference area. The reference length used for computing the pitching moment coefficient was the geometric mean chord length, S/b, for the main wing.

The moment coefficient shown in Fig. 11 is for the pitching moment about the reference origin. Thus we see that, with the center of gravity located at this reference origin, there would be a stable trim

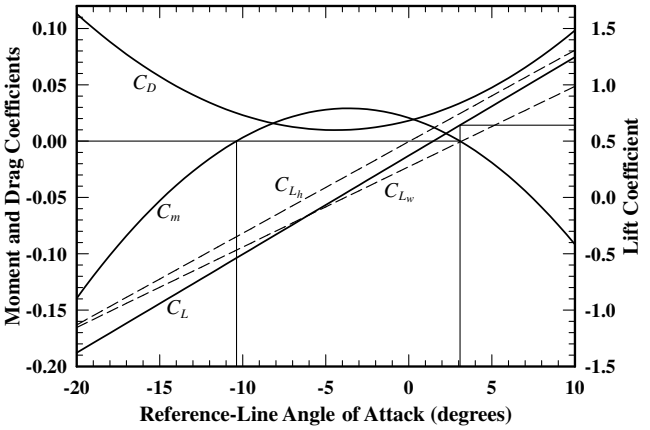

Fig. 11 Aerodynamic coefficients vs angle of attack for example wing–canard configuration, with the pitching moment origin located on the fuselage reference line 4.0 ft below the main wing.

point (i.e., $C_m = 0.0$) at an angle of attack of approximately 3.1 deg corresponding to a lift coefficient of about 0.64. However, due to the highly nonlinear pitching moment about this c.g. location, we also see that a large negative disturbance in angle of attack (i.e., one producing a reference-line angle of attack less than −10.4 deg) would result in a divergent pitching moment. This phenomenon is due almost entirely to the vertical offset between the aerodynamic center and the center of gravity.

The location of the aerodynamic center of this wing–canard configuration, at any given angle of attack, can be determined from the results plotted in Fig. 11 by using Eqs. (37–39) in Eqs. (29) and (30). With the required first and second derivatives approximated using second-order central difference and angle of attack increments of 0.5 deg, the results plotted in Fig. 12 were obtained. Notice that the variation in the position of the aerodynamic center over this wide range of angle of attack is very slight, with the x coordinate ranging from 0.15 to 0.19 ft aft of the origin and the y coordinate ranging from 3.02 to 3.31 ft above the origin. For comparison, Fig. 12 also shows the x coordinate of the aerodynamic center as predicted from the traditional approximation given by Eq. (61) as well as the x and y coordinates predicted from Eqs. (80) and (81).

To demonstrate that the nonlinear pitching moment shown in Fig. 11 results primarily from the vertical offset between the aerodynamic center and the pitching moment origin, the computations used to obtain Fig. 11 were repeated with the pitching moment origin moved to the coordinates $x = 0.00$ and $y = 3.26$ ft, which corresponds to the vertical coordinate obtained from Eq. (81). With only this change, the results shown in Fig. 13 were obtained. Thus, we see that the undesirable stability characteristic shown in Fig. 11 can be eliminated by vertically aligning the center of gravity with the aerodynamic center of the aircraft.

Although it is relatively uncommon, if the center of gravity of an airplane were located substantially above its aerodynamic center, the trigonometric and aerodynamic nonlinearities would again have a detrimental effect on the pitch-stability characteristics of the aircraft. This is demonstrated here by repeating the computations used to obtain Figs. 11 and 13, but with the pitching moment origin moved to the coordinates $x = 0.00$ and $y = 6.50$ ft, which is approximately 3.25 ft above the aerodynamic center. These results are shown in Fig. 14. Notice that, if the center of gravity were located at this point, there would be a barely stable trim point at an angle of attack of approximately −0.5 deg corresponding to a lift coefficient of about 0.33. However, a positive disturbance in angle of attack of only about 3.2 deg would result in a divergent pitching moment. This is very different from the pitch-stability characteristics that were observed with the center of gravity located either at or below the vertical level of the aerodynamic center.

By comparing Figs. 11, 13, and 14, we see that the pitch-stability characteristics of an airplane can be profoundly altered by changing the vertical position of the center of gravity relative to the aerodynamic center without changing the axial static margin. This demonstrates the critical importance of being able to predict the vertical position of the aerodynamic center of an airplane as well as its axial position. From Fig. 11 we see that, when the center of gravity is below the aerodynamic center, the nonlinearities are stabilizing at positive angles of attack but become extremely destabilizing at large negative angles of attack. Figure 14 shows that just the opposite characteristics prevail when the center of gravity is above the aerodynamic center. In Fig. 13 we see little variation in pitch stability with angle of attack when the center of gravity is vertically aligned with the aerodynamic center.

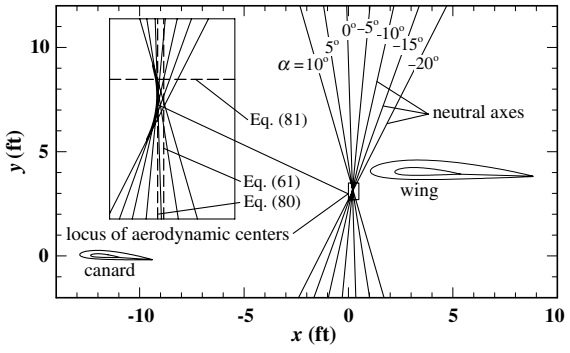

Fig. 12 Locus of aerodynamic centers for the example wing–canard configuration.

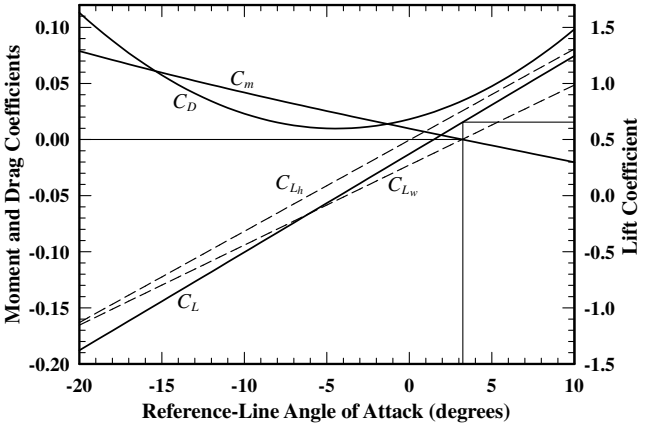

Fig. 13 Aerodynamic coefficients vs angle of attack for the example wing–canard configuration, with the pitching moment origin located 3.26 ft above the fuselage reference line and 0.74 ft below the main wing.

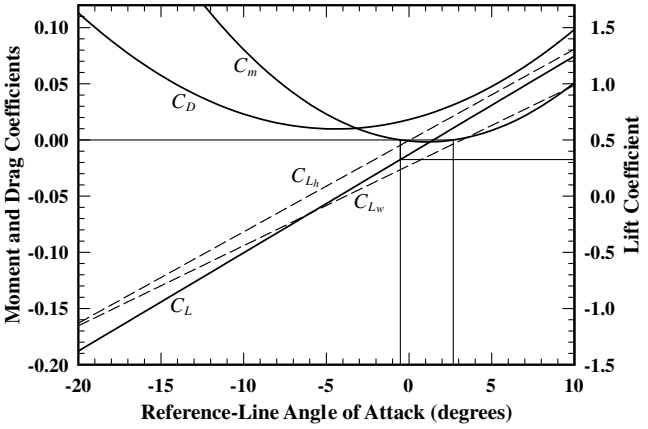

Fig. 14 Aerodynamic coefficients vs angle of attack for the example wing–canard configuration, with the pitching moment origin located 6.50 ft above the fuselage reference line and 2.50 ft above the main wing.

To demonstrate how drag contributes to the stability characteristics of this wing–canard configuration, results similar to those shown in Figs. 11 and 12 were obtained using the zero-drag approximation given by Eqs. (62–64). These results are shown in Figs. 15 and 16. For comparison the pitching moment obtained from Eq. (39), including the effects of drag, is also shown in Fig. 15. Notice that, for this high-wing configuration, drag is destabilizing for positive lift and stabilizing for negative lift. Thus, drag reduces the nonlinearity in the pitching moment curve.

There are other nonlinearities, which are not accounted for in the two-lifting-surface model presented here. In reality, the downwash induced on one lifting surface by another is not exactly a linear function of lift. For example, the downwash induced on the wing by the canard is extremely complex, varying from positive near the wing root to negative in the regions outboard from the tip vortices shed by the canard. Not only does the downwash vary over the span of the wing, but the downwash gradient changes with angle of attack, due to the fact that the canard vortices pass closer to the wing at the higher angles of attack. The numerical lifting-line method presented by Phillips and Snyder [15] is capable of capturing these additional nonlinearities. Results obtained from such computations are presented in Figs. 17 and 18.

We see from Fig. 17 that, at the higher angles of attack, the numerical lifting-line method predicts a decrease in pitch stability relative to the results obtained from the closed-form model presented here. This is a consequence of the fact that the downwash gradient on the wing increases with increasing angle of attack, because the canard vortices pass closer to the wing. This increased downwash gradient reduces the stabilizing contribution from the aft wing. However, the difference between the numerical lifting-line results and Eq. (39) is small. Furthermore, for this example with no sweep, both the numerical lifting-line solution and the closed-form model predict only slight variations in the position of the aerodynamic center with angle of attack. As was shown in our first example, much larger variations in the vertical position of the aerodynamic center with angle of attack should be expected for geometries with substantial sweep.

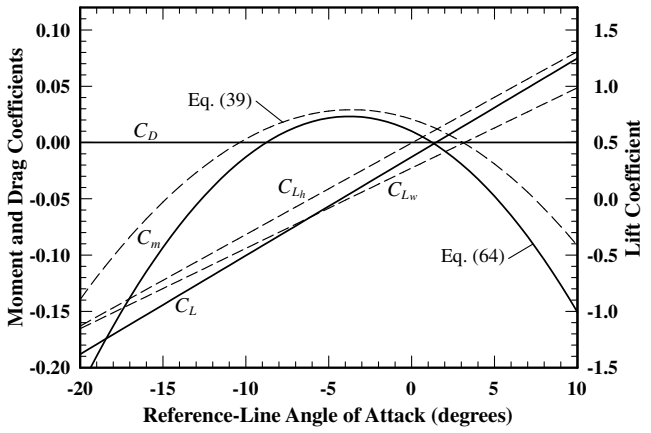

Fig. 15 Aerodynamic coefficients vs angle of attack for the example wing–canard configuration as estimated neglecting the effects of drag.

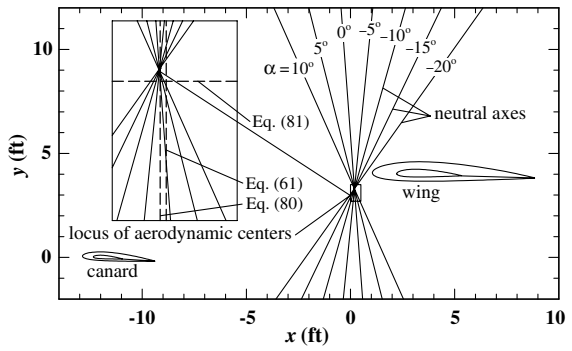

Fig. 16 Locus of aerodynamic centers for the example wing–canard configuration as estimated neglecting the effects of drag.

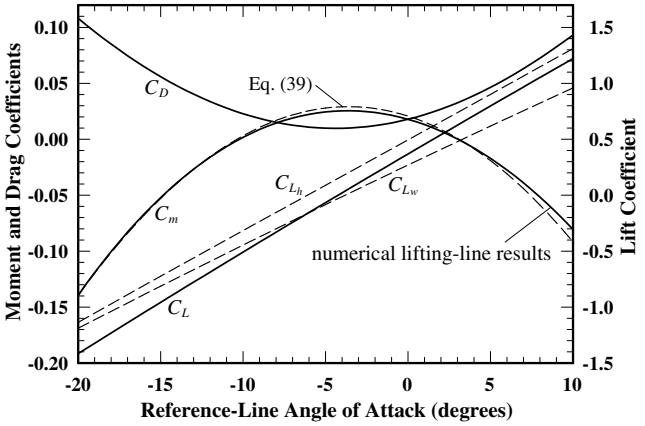

Fig. 17 Aerodynamic coefficients vs angle of attack for the example wing–canard configuration as predicted from numerical lifting-line computations.

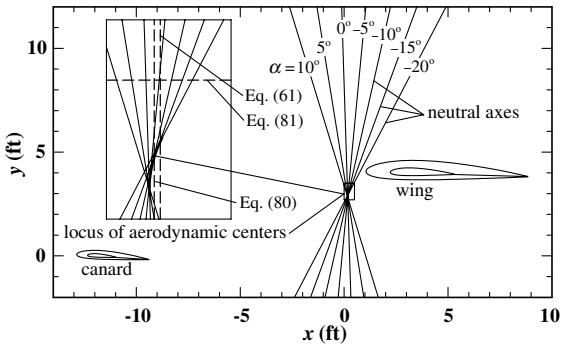

Fig. 18 Locus of aerodynamic centers for example wing–canard configuration as predicted from numerical lifting-line computations.

Conclusions

The aerodynamic center of a wing or complete aircraft is traditionally defined to be the point about which the pitching moment is independent of the angle of attack. The traditional method for estimating the position of the aerodynamic center neglects the nonlinearities associated with the trigonometric functions and the drag and provides an estimate for only the axial coordinate of the aerodynamic center. However, outside the approximation of linear aerodynamics, there exists no fixed point on a wing or complete aircraft about which the pitching moment is completely independent of the angle of attack. Additionally, trigonometric and aerodynamic nonlinearities can have a significant effect on aircraft stability. Furthermore, because vertical offset between the aerodynamic center and the center of gravity can have a profound effect on an airplane's response to large disturbances in the angle of attack, it can be important to know both the axial and vertical coordinates of the aerodynamic center of an aircraft as determined with the nonlinearities included.

The refined mathematical definition for the aerodynamic center, which is given by Eqs. (1) and (2), leads to the general relations for the location of the aerodynamic center that are given by Eqs. (29) and (30). In all cases, the plane of symmetry for a wing or complete aircraft contains an infinite number of points about which the change in pitching moment with respect to angle of attack is zero. The locus of such points is always a straight line, which has been referred to here as the neutral axis. With small changes in angle of attack, the neutral axis rotates about the aerodynamic center as shown in Figs. 6,

12, 16, and 18. When drag is neglected and the traditional approximation of linear aerodynamics is applied to Eq. (29), the traditional approximation for the axial position of the aerodynamic center is recovered. Furthermore, under an improved linear approximation, Eqs. (29) and (30) provide simplified relations for both the axial and vertical positions of the aerodynamic center, as given by Eqs. (80) and (81). In the more general case of nonlinear aerodynamics including the effects of drag, Eqs. (29) and (30) show that the aerodynamic center is uniquely defined only for small perturbations about any given angle of attack.

When the effects of trigonometric and aerodynamic nonlinearities are combined with wing sweep at high angles of attack below stall, the aerodynamic center of a planar wing moves significantly aft and below the plane of the wing, producing a substantial destabilizing effect on the wing. For airplanes without highly swept wings, the variation in the position of the aerodynamic center caused by the nonlinear effects is small. However, if the center of gravity of an airplane is substantially above or below the aerodynamic center, nonlinear effects can have a detrimental effect on pitch stability by producing large variations in the pitch-stability derivative with angle of attack, as shown in Figs. 11, 14, 15, and 17. These variations in the pitch-stability derivative can be all but eliminated by keeping the center of gravity in close vertical alignment with the aerodynamic center of the airplane, as is shown in Fig. 13.

Acknowledgments

The CFD computations for this work were performed on the Uinta supercomputer, which was provided by the National Science Foundation under grant number CTS-0321170 with matching funds provided by Utah State University. The authors would like to acknowledge the computer time donated by the Center for High Performance Computing at Utah State University.

References

[1] Etkin, B., and Reid, L. D., "Lift and Pitching Moment of the Wing," and "Mean Aerodynamic Chord, Mean Aerodynamic Center, and $C_{m_{ac}}$," *Dynamics of Flight: Stability and Control*, 3rd ed., Wiley, New York, 1996, pp. 24–25 and 357–363.

[2] McCormick, B. W., "Aerodynamic Center Location for a Finite Wing, $C_{m_{ac}}$, and Mean Aerodynamic Chord (MAC)," *Aerodynamics, Aeronautics, and Flight Mechanics*, 2nd ed., Wiley, New York, 1995, pp. 126–128.

[3] Pamadi, B. N., "Concept of Aerodynamic Center," and "Stick-Fixed Neutral Point," *Performance, Stability, Dynamics, and Control of Airplanes*, 2nd ed., AIAA, Reston, VA, 2004, pp. 20–22 and 202–204.

[4] Raymer, D. P., "Wing Geometry," *Aircraft Design: A Conceptual Approach*, 2nd ed., AIAA, Washington, D.C., 1992, pp. 47–65.

[5] Krist, S. L., Biedron, R. T., and Rumsey, C. L., "CFL3D Users Manual (Ver. 5)," NASA TM-1998-208444, June 1998.

[6] Spalart, P., and Allmaras, S., "A One-Equation Turbulence Model for Aerodynamic Flows," AIAA Paper 1992-0439, Jan. 1992.

[7] Alley, N. R., Phillips, W. F., and Spall, R. E., "Predicting Maximum Lift Coefficient for Twisted Wings Using Computational Fluid Dynamics," *Journal of Aircraft*, Vol. 44, No. 3, 2007, pp. 911–917. doi:10.2514/1.25643

[8] Richardson, L. F., "The Approximate Arithmetical Solution by Finite Differences of Physical Problems Involving Differential Equations, with an Application to the Stresses in a Masonry Dam," *Transactions of the Royal Society of London, A*, Vol. 210, Jan. 1910, pp. 307–357.

[9] Richardson, L. F., and Gaunt, J. A., "The Deferred Approach to the Limit," *Transactions of the Royal Society of London, A*, Vol. 226, Jan. 1927, pp. 299–361.

[10] Phillips, W. F., Fugal, S. R., and Spall, R. E., "Minimizing Induced Drag with Wing Twist, Computational-Fluid-Dynamics Validation," *Journal of Aircraft*, Vol. 43, No. 2, 2006, pp. 437–444. doi:10.2514/1.15089

[11] Kuethe, A. M., and Chow, C. Y., "The Twisted Wing: Basic and Additional Lift," *Foundations of Aerodynamics*, 5th ed., Wiley, New York, 1998, pp. 188–199.

[12] Phillips, W. F., Hunsaker, D. F., and Niewoehner, R. J., "Estimating the Subsonic Aerodynamic Center and Moment Components for Swept Wings," *Journal of Aircraft*, Vol. 45, No. 3, 2008, pp. 1033–1043. doi:10.2514/1.33445

[13] McCormick, B. W., "Downwash Angle," *Aerodynamics, Aeronautics, and Flight Mechanics*, 2nd ed. Wiley, New York, 1995, pp. 479–482.

[14] Phillips, W. F., "Estimating the Downwash Angle on an Aft Tail," *Mechanics of Flight*, Wiley, Hoboken, NJ, 2004, pp. 371–381.

[15] Phillips, W. F., and Snyder, D. O., "Modern Adaptation of Prandtl's Classic Lifting-Line Theory," *Journal of Aircraft*, Vol. 37, No. 4, 2000, pp. 662–670.